# Material Dependence on Plasma Shielding Induced by Laser Ablation*)

Takuya KONO, Akinori ISHIKAWA[1)], Seigo MISAKI, Atsushi SUNAHARA[2)], Satoshi TANAKA[1)], Toshinori YABUUCHI, Yoshi HIROOKA[3)] and Kazuo A TANAKA

*Graduate School of Engineering, Osaka University, Suita, Osaka 565-0871, Japan*
[1)]*Department of Media Technology, Ritsumeikan University, Kusatsu, Shiga 525-8577, Japan*
[2)]*Institute for Laser Technology, 2-6 Yamadaoka, Suita, Osaka 565-0871, Japan*
[3)]*National Institute for Fusion Science, Toki, Gifu 509-5292, Japan*

(Received 9 December 2011 / Accepted 28 March 2012)

Plasma shielding is an important concept to study if the material damage could be suppressed with plasma layer properly prepared by absorbing the incoming plasma flux onto a divertor target in MFE or the first wall in IFE reactors. First experimental evidence of this effect is reported. Two plasma plumes ($n \sim 10^{12}$/cm$^3$, $T_e \sim 1$ eV) are created with two laser beams. The laser ablation plasma plumes are created at laser energy density up to 10 J/cm$^2$ and are crossed each other. 12~59 % of the incoming plasma particles are shielded with the collisions of the other plasma plume. By observing the material dependence of colliding effects, the effect to plasma shielding is discussed.



Keywords: plasma shielding, vapor shielding, laser ablation, plasma collision, IFE first wall, MFE divertor

DOI: 10.1585/pfr.7.2405065

## 1. Introduction

In the fusion reactor research, it is one of the important theme how to study suppress the damage on plasma facing components (PFC). For example, expected heat loads are 10 to 100 MW/m$^2$ at the magnetic fusion energy (MFE) divertor at ELM and disruptions, and $10^{13}$ W/m$^2$ or even higher at the inertial fusion energy (IFE) first walls. The values of the heat fluxes could be beyond the ablation threshold of any solid or liquid material. The PFCs appear subject to material ablation. However active functions in plasmas are proposed to protect PFC such as vapor shielding [1, 2] and plasma shielding effects. Our intention is to shed light on this effect using active experimental platform based on high repetition (10 Hz) laser system. The laser system can deliver the heat flux mentioned above relatively easily. In addition the dynamic range of the heat flux can be varied in the many orders of magnitude for the parametric study. The density and temperature are also the factors of interest and can be controlled in this platform.

To study the issues of PFC under an extreme heat flux, it is useful to observe how the ablated plasma behaves in the experimental platform which simulates MFE divertor or IFE chamber wall with the cylindrical structure. In previous studies by K.A. Tanaka and Y. Hirooka, the first series of plasma interaction experiments were performed [3–5]. Plasma plumes created by laser ablation collide and change the direction for the case of Carbon plumes. The plumes appear cross each other for the case of Tungsten. Apparent behavior is totally different for the two cases. It will be shown in the following that this difference is actually closely related to the characteristics of plasma shielding.

## 2. Experimental Setup

Plasma shielding is studied using the experimental setup "LEAF-CAP" (Laboratory Experiments on Aerosol Formation by Colliding Ablation Plumes) [3, 4]. Figure 1 (a) shows the setup, a third harmonic beam of Nd: YAG laser (355 nm, 6 ns, 10 Hz) is optically split into equal-power. Each beam is line-focused to 0.1 mm × 10 mm focal shape. Two concave targets are ir-

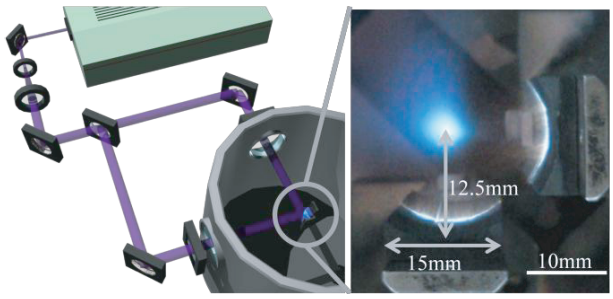


(a) (b)

Fig. 1 Experimental setup "LEAF-CAP". (a) Laser and experimental chamber, (b) Inside view of LEAF-CAP in case of Carbon targets.

*author's e-mail: kono-t@eie.eng.osaka-u.ac.jp*
*) This article is based on the presentation at the 21st International Toki Conference (ITC21).

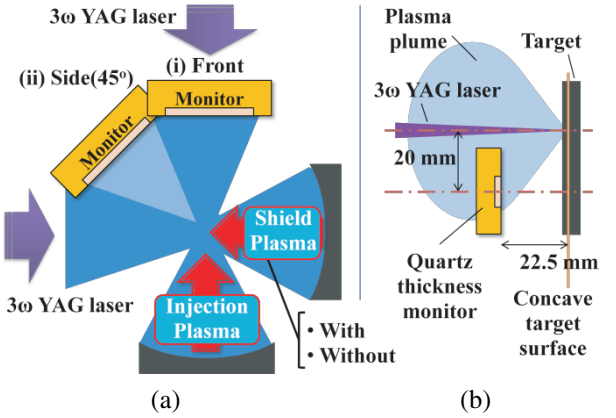


Fig. 2 Setting of quartz thickness monitors, (a) top view, (b) side view. Two quartz thickness monitors are placed to measure the injection plasma with or without the shield plasma.

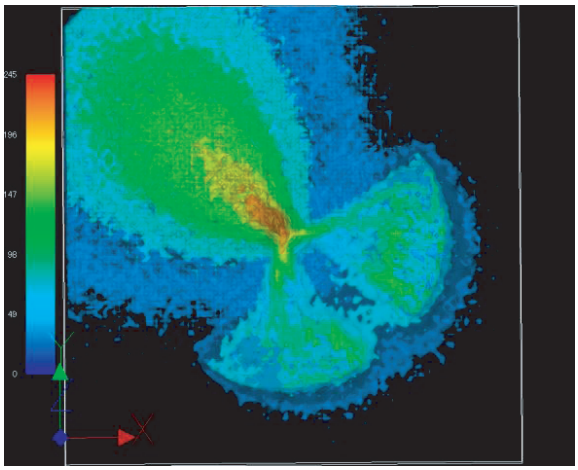

Fig. 3 Radiation behavior of Carbon plasma plumes. The image processing has been used to integrate the 100 frames of fast 2D images taken with a 50 ns time frame.

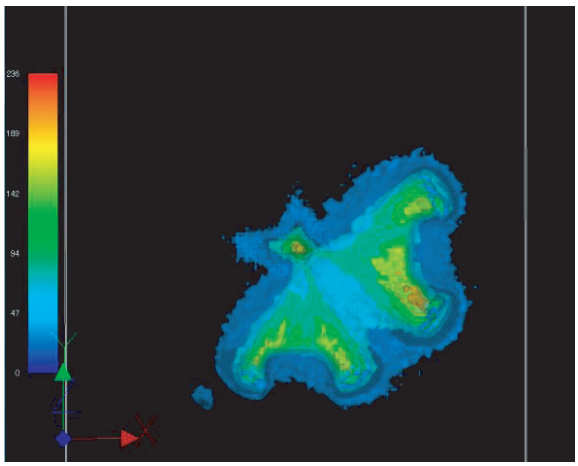

Fig. 4 Radiation behavior of Tungsten plasma plumes.

radiated with the two orthogonally oriented laser beams at room temperature in a vacuum chamber ($\sim 10^{-3}$ Pa). Carbon, Aluminum, Copper, Molybdenum and Tungsten are used as the targets. The ablated plasma plumes cross each other at 12.5 mm from the surfaces with focusing caused by the concave target structure (Fig. 1 (b)). The line-focused laser energy density is 10 J/cm$^2$/pulse. The plasma density is $\sim 10^{18}$/m$^3$ and the temperature is $\sim 1$ eV measured with a Langmuir probe [5]. Our purpose here is to understand the plasma collision and energy transfer processes. The parameter range is somewhat close, but not exactly matched to the extreme conditions expected at the vicinity of divertor targets. As mentioned in ref. [5], it is possible to create extreme conditions matched to the ones at the divertor. This is left as a future issue.

To observe the behavior of ablated plasma, an intensified CCD (ICCD) camera (ANDOR Technology) is placed at the top of vacuum chamber. In our experimental setup, the camera can detect the visible light in the range between 390 and 850 nm. Fast 2D images of the colliding plumes can be taken at any desired timing by controlling the trigger delay.

Two quartz thickness monitors are set to measure the number of plasma particles at (i) front and (ii) side (45°) as shown in Fig. 2. As seen in Fig. 2 (b) side view, the laser beams irradiate the targets without hitting the thickness monitors. The plasma plume expands in the vertical direction and focus in the horizontal direction. The depositions at each place are compared with and without the shield plasma. A quartz thickness monitor has a quartz crystal unit (diameter: 10 mm) and measures coat speed (Å/s) of coming in particles.

## 3. Results and Discussion

### 3.1 Observation with ICCD camera

The behavior of ablated plasma is observed with ICCD camera. Carbon and Tungsten are used as the targets. The temporal frame is 50 ns for observing the plasma emission. Each frame is taken at every 50 ns with a different trigger delay for 5 μs (100 frames) in 100 independent shots. Since the behaviors of plumes are reproducible, the entire frames can be integrated into a single figure after a proper image processing. The integrated images are shown in Fig. 3 (Carbon) and Fig. 4 (Tungsten). The relative value of radiation intensity is shown in the figure with the color bars. Based on another spectroscopic study the emission from the Carbon collision and stagnation are dominated with the Carbon Swan band: the sign of Carbon molecular formation [3]. The radiation increase indicates that the effective molecular formation takes place due to the plasma interaction. In case of Carbon, one can see that two plasma plumes ablated from two targets collide each other at the cross point and the radiation appears to stagnate for 3-4 μs after the collision starts. This temporal duration could be related closely to the temporal width of plumes. Then the radiation appears to move at 45°. In case of Tungsten, the

Table 1 Results of quartz thickness monitor (Carbon).

| | | At front (0°) (Å/s) | At side (45°) (Å/s) | Fraction toward 45° monitor |
|---|---|---|---|---|
| Coat speed | Without | 15 | 0.21 | 1.4% |
| | With shield plasma | 6.1 | 2.7 | 31% |
| Shielded rate | | 59% | - | - |
| Fractional Increase toward 45° monitor | | - | - | 30 points |

Table 2 Results of quartz thickness monitor (Tungsten).

| | | At front (0°) (Å/s) | At side (45°) (Å/s) | Fraction toward 45° monitor |
|---|---|---|---|---|
| Coat speed | Without | 1.0 | 0.0091 | 0.90% |
| | With shield plasma | 0.88 | 0.064 | 6.8% |
| Shielded rate | | 12% | - | - |
| Fractional Increase toward 45° monitor | | - | - | 5.9 points |

plume radiation runs right after the cross point. Just by observing the self-emission it may be difficult to judge if the Tungsten plumes collide and change the direction since the emission may not be strong enough from cold plumes.

## 3.2 Observation with quartz thickness monitor

Table 1 shows the result of the quartz thickness monitor at each place with and without the shield plasma in case of Carbon targets. Without the shield plasma, the coat speed is 15 Å/s at the front (0°) monitor and 0.21 Å/s at the side (45°). The side accounts 1.4 % of the total.

On the other hand with the shield plasma, the coat speed at the side is 5.4 Å/s. It should be noted that the side counts contribution from two plasma plumes in this case. Therefore, in case with the shield plasma, the side value should be multiplied by a factor 0.5. After this correction, the coat speed at the side is 2.7 Å/s, 12.6 times increase compared to the one without the shield. The front shows 6.1 Å/s. The side accounts 31 % of the total. This value indicates that 59 % of the plasma particles are shielded.

From these measured values, the shield plasma functions to reduce the incoming plasma flux. As the result of the collision, the fraction toward 45° monitor increases by 30 points.

The results in case of Tungsten are shown in Table 2. Tungsten is a candidate material for the divertor and the first wall. Without the shield plasma, the coat speed is 1.0 Å/s at the front and 0.0091 Å/s at the side. The side accounts 0.90 % of the total. With the shield plasma, the corrected side shows 0.064 Å/s, 7.0 times increase compared to the ones without the shield. The front shows 0.88 Å/s, indicating 12 % shielding. The side accounts 6.8 % of the total. While 30 points increase is observed at the side for Carbon, 5.9 points increase is observed for Tungsten.

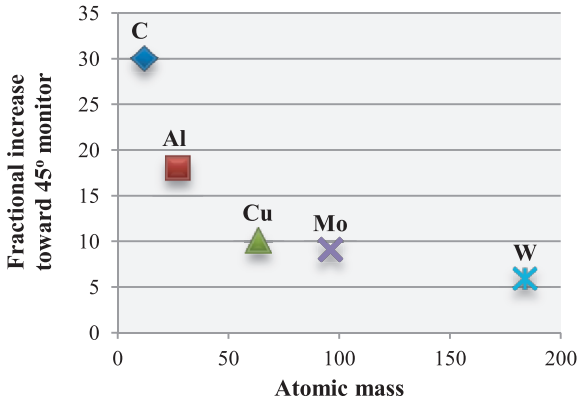


Fig. 5 Atomic mass vs. Fractional increase of deposition at the side.

We have observed that the fractions increased at the side with the shield plasma for all materials: C, Al, Cu, Mo, and W. The material dependence of the fractional increase is summarized in Fig. 5. The result indicates clearly that the plumes change the direction more effectively with a small atomic mass.

## 3.3 Collision parameter

We discuss now the material dependence of the collision behaviors. In our plasma state ($n \sim 10^{12}/\mathrm{cm}^3$, $T_e \sim 1$ eV), it is estimated that the elastic collision by neutral particles may be less likely to take place but Coulomb collision by ion particles is dominant [6]. We define now a collision parameter for further understanding.

In a theoretical model of plasma interaction between $\alpha$ and $\beta$ species, the variance of Coulomb collision is given by Eq. 1 [7],

$$\langle \delta^2 \rangle = \left( \frac{q_\alpha^2 q_\beta^2 n_L \lambda}{8\pi\epsilon_0^2 m_{\alpha\beta}^2 u^3} \right) \Delta t, \tag{1}$$

where $\Delta t$ s is the time interval, $\epsilon_0$ ($\mathrm{m}^{-3}\,\mathrm{kg}^{-1}\,\mathrm{s}^4\,\mathrm{A}^2$) is the permittivity of vacuum, $n_L$ ($\mathrm{m}^{-3}$) is the lower density of either $n_\alpha$ or $n_\beta$, and $\lambda$ denotes the Coulomb logarithm. To consider the collision effects in different materials, we consider the probability of collision that is a function of the charge state of ion $q_\alpha$, $q_\beta$ (A·s), the reduced mass $m_{\alpha\beta}$ ($= m_\alpha m_\beta/(m_\alpha + m_\beta)$) (kg) and the relative velocity $u$ ($\mathrm{m \cdot s}^{-1}$). Then, the probability is expressed as the collision parameter (CP):

$$CP = \frac{\sum_i i^4 f_i}{m^2 u^3} \quad (i = 1, 2, \cdots). \tag{2}$$

In Eq. 2, $i^4$ is a weight corresponding to a charge state of the ion. When the charge states are 1 and 2, the values $i^4$ become 1 and 16. This term indicates the sensitivity on the

Table 3 Collision parameter (normalized to Tungsten).

| | $m$ | $u$ (m/s) | $f_0$ | $f_1$ | $f_2$ | $\sum_i i^4 f_i$ | Collision Parameter |
|---|---|---|---|---|---|---|---|
| **C** | 12 | $3.1\times10^4$ | 0.3 | 0.7 | 0 | 0.70 | 83 |
| **Al** | 27 | $2.9\times10^4$ | 0 | 1.0 | 0 | 1.0 | 29 |
| **Cu** | 64 | $2.6\times10^4$ | 0.3 | 0.6 | 0.1 | 2.2 | 15 |
| **Mo** | 96 | $1.8\times10^4$ | 0.7 | 0.3 | 0 | 0.30 | 2.9 |
| **W** | 184 | $1.6\times10^4$ | 0.7 | 0.3 | 0 | 0.30 | 1.0 |

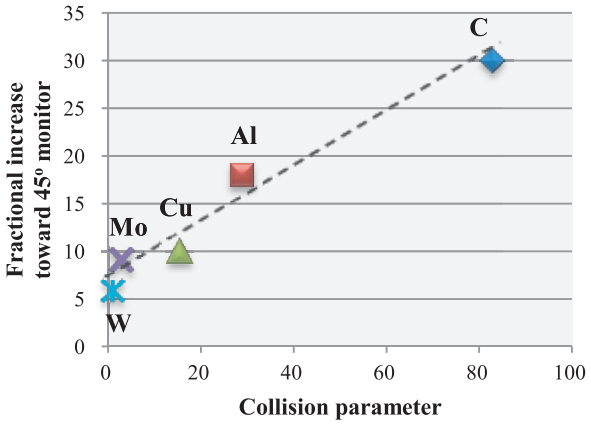


Fig. 6 Collision parameter vs. Fractional increase of deposition at the side.

collision behavior with the ion charge states. A fraction of ions with the charge state of $i$ is expressed as $f_i$. The fractions are estimated from the database of Atomic Molecular Data Services [8] depending on the plasma density and temperature. The velocity $u$ is taken from the velocity of plasma radiation observed with the ICCD camera. The parameters used to estimate the CP is shown in Table 3 as values normalize to the Tungsten.

The CP is compared with the experimental results. As shown in Fig. 6, the collision parameter is linearly correlated with the fractional increase at the side in our experiment. This result indicates that the CP could be a useful index parameter to estimate plasma collision behavior.

# 4. Conclusion

Plasma shielding effect has been studied using laser ablation method: LEAF-CAP for understanding the ablated plasma behaviors for PFC. When an injection plasma plume is intersected with another shield plasma, the cross point is monitored with ICCD camera at a 50 ns frame speed for entire plume histories.

The quartz thickness monitor reads the incoming flux of the plasma plume either with or without the shield plasma. 60 % of the Carbon injection plasma is found to be shielded. The fraction varied with materials. The plasma shielding is effective for small atomic mass plasmas under our current experimental conditions.

We have defined the collision parameter. The collision parameter consists of the charge state of ion, mass and velocity and shows a linear correlation with the shielding effect. The parameter could be used to estimate the plasma collision behaviors.

# Acknowledgments

This research is supported by LHD project collaborative research: NIFS10KOAF001 at National Institute of Fusion Science. A part of this research is supported by JSPS “ASHULA” Asia research education project.

[1] J.G. van der Laan, M. Akiba, A. Hassanein, M. Seki and V. Tanchuk, Fusion Eng. Des. **18**, 135 (1991).
[2] A.M. Hassanein, G.L. Kulcinski and W.G. Wolfer, Nucl. Eng. Des./Fusion **1**, 307 (1984).
[3] Y. Hirooka, K.A. Tanaka, H. Sato, K. Ishihara and A. Sunahara, J. Phys. Conf. Ser. **244**, 032033 (2010).
[4] Y. Hirooka, T. Oishi, H. Sato and K.A. Tanaka, Fusion Sci. Technol. **60**, 804 (2011).
[5] K.A. Tanaka, A. Hassanein, Y. Hirooka, T. Kono, S. Misaki, T. Ohishi, A. Sunahara and S. Tanaka, Fusion Sci. Technol. **60**, 329 (2011).
[6] S. Misaki, A. Sunahara, T. Kono, T. Yabuuchi and K.A. Tanaka, APS-DPP, 53rd Ann. Meet., UP9.00090 (2011).
[7] T. Takizuka and H. Abe, J. Comput. Phys. **25**, 205 (1977).
[8] Atomic Molecular Data Services, IAEA, http://www-amdis.iaea.org/FLYCHK/